Pirvan, Petrisor-Alin (2019) *Development of aliphatic thiosulfonates as cysteine protease inhibitors.* MSc(R) thesis.

Development of aliphatic thiosulfonates as cysteine protease inhibitors

Petrisor-Alin Pirvan

Supervisors: 1st – Robert Liskamp, 2nd – Joëlle Prunet

Submitted in fulfilment of the requirements for the Degree of MSc by Research

School of Chemistry

College of Science and Engineering

University of Glasgow

June 2019

Abstract:

Cysteine proteases are implicated in a wide range of biological processes, which makes them an important factor in the pathogenesis of many diseases. Dysregulation of protease activity can lead to various diseases such as cancer, osteoporosis, neurological disorders and cardiovascular diseases. Furthermore, cysteine proteases have been proved to play a critical role in the life cycle of parasitic infections, an issue that grows every year due to increasing human migration. Therefore, cysteine proteases show great potential as targets for medicinal chemists.

The following work aims to address this area of research through the synthesis of non-natural amino acid derived thiosulfonate warheads.

Table of Contents:

List of Figures:

List of schemes:

List of abbreviations:

Boc: N-tert-butoxycarbonyl

CDC: Centre for disease control

DCM: Dichloromethane

DiPEA: N,N-diisopropylethylamine

DMF: N,N-Dimethylformamide

DMSO: Dimethyl sulfoxide

MeCN: Acetonitrile

MMTS: Methyl Methanethiosulfonate

TBDMS: tert-Butyldimethylsilyl Ether

TFA: Trifluoroacetic acid

THF: Tetrahydrofuran

WHO: World Health Organisation

1 Introduction

1.1 Motivation:

Proteases are a large family of peptide-bond hydrolysing enzymes. They are present in all eukaryotic organisms and regulate a vast number of processes such as cell death, proliferation, migration and protein turnover.[1] Dysregulation of these proteolytic enzymes can lead to the disruption of the biological processes they control.

Among these enzymes, cysteine proteases have been recognised as causal agents in human pathologies.[2] Furthermore, cathepsins have an essential role in the infectivity and life cycle of protozoa such as *Plasmodium falciparum* (Malaria), *Trypanosoma brucei* (African sleeping sickness) and *Trypanosoma cruzi* (Chagas disease), making them promising drug targets.[3]

1.2 Active site and structure:

Proteases hydrolyse peptide bonds and can be classified into five major classes: aspartic, threonine, serine, cysteine and metalloproteases.[1] All papain-like cysteine proteases are composed of a left (-L) and a right (-R) domain. The L-domain contains three α-helices while the R-domain is a β-barrel closed at the bottom by a α-helix. The two domains form a cleft in the middle where the active site is situated.[4] Cysteine proteases are characterised by their highly conserved active site consisting of a cysteine, histidine and asparagine residue[1] (figure 1).
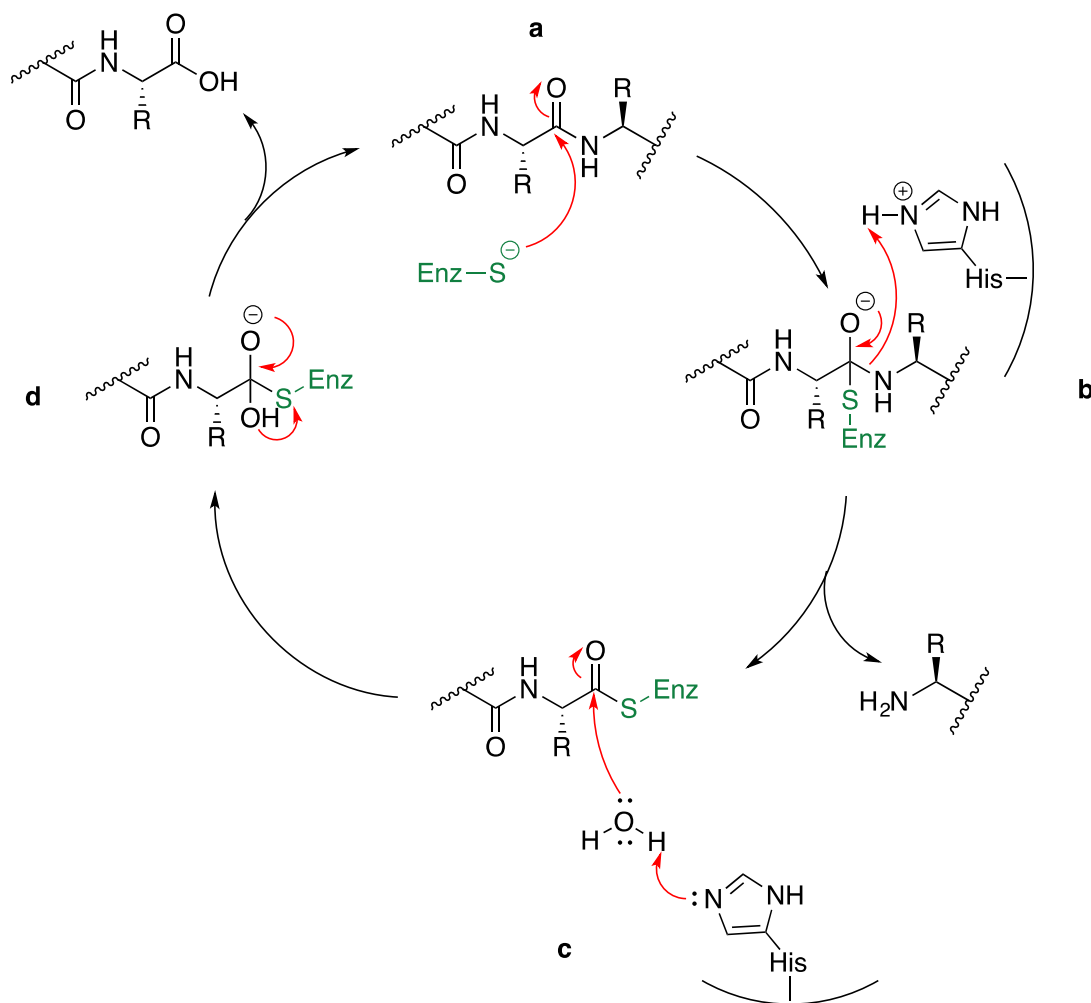
Figure 1: Catalytic cycle of cysteine protease active site.

Cys[25] and His[159] are thought to be catalytically active as a thiolate-imidazolium ion pair.[1] The Asn[175] forms a hydrogen bond to the His159 imidazole and orientates it in the optimum positions for various steps of the catalytic mechanism. The nucleophilic active site thiol can attack the carbonyl of the scissile bond (Figure 1, **a**) and form a tetrahedral intermediate (Figure 1, **b**) which collapses yielding a thioester (Figure 1, **c**). The thioester finally gets hydrolysed to yield the carboxylic acid and the active site nucleophilic thiol. [4] By contrast, other enzymes such as serine and threonine proteases have a nucleophilic oxygen in their active site. This key distinction can be used when designing a specific inhibitor that can differentiate between enzyme classes and interact only with the active site thiol of cysteine proteases.

According to the nomenclature of Schecter and Berger[5] there are seven subsites in the binding area of cysteine proteases. Four on the acyl side (S4, S3, S2, S1) and

three (S1', S2', S3') on the amino side of the scissile bond (Figure 2). The S2, S1 and S1' subsites are the three well defined sites where residues can interact with the enzyme by both their main and side chain. It is worth noting that the S2 binding site is the largest and most defined in papain cysteine proteases and thus the interaction between the S2 site and the complementary P2 residue is key in determining inhibitor specificity.[6]
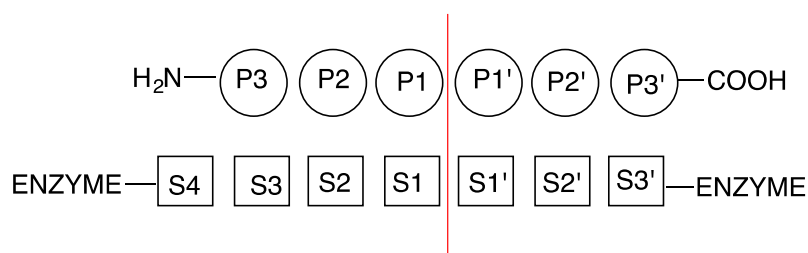

Figure 2: Representation of enzyme-substrate complex and the seven binding subsites.

Cathepsins are proteases found in all animals and most other organisms. Most of the members of this group become activated at low pH and their activity lies almost entirely within the acidic environment of the lysosomes. There are 11 cysteine cathepsins expressed in the human genome[1]. Most cathepsins have structures composed of two domains (left and right domain) and the active site cleft in the middle. Depending where they cleave their substrates, cathepsins can be classified as exopeptidases (Cathepsin B, C and X) or endopeptidases (Cathepsin L, F and K).[6] A typical feature cathepsin B-like cysteine proteases is the existence of an occluding loop between conserved Pro-Tyr[103] motif and Cys[128]. This loop contains two histidine residues (His[110] and His[111]) which anchor the C-terminal carboxyl group of peptide and protein substrates and are responsible for the dipeptidyl carboxypeptidase activity of the enzyme (removes C-terminal dipeptides)[7]. Cathepsin L has an endopeptidase activity and will selectively cleave peptides with aromatic residues in the P2 position and hydrophobic residues in the P3 position.[8] These differences can be exploited to design a more specific inhibitor that can target individual cysteine proteases.

1.3 Cysteine proteases in cancer:

The broad range of the biological processes that cathepsins are involved in indicates their importance within the organism. Aberrant cathepsin activity has been shown to

contribute to many diseases such as: osteoporosis, arthritis, obesity, cystic fibrosis, many types of cancer and parasitic pathogenesis.[9]

In many cancer types, increased levels of cathepsins correlate to increased malignancy. Dysregulation of cysteine protease activity is crucial for tumourgenesis. Cathepsins recycle proteins for cancer cell survival and proliferation, and they modify tumour microenvironment which leads to invasion and disease progression. They also contribute to activation of growth factors, immune system regulation and metastasis. Therefore, cysteine cathepsins represent an important class of proteins that facilitate cancer progression.[10]

The attempt of cancer treatment via protease inhibition was done via matrix metalloproteases (MMPs) [11]. However, MMPs failed in clinical trials which led to the termination of their use. These molecules reached phase III in clinical trials but were terminated due to their activity against both pro and anti-tumorigenic proteases. Furthermore, they proved to be effective only against early stages of cancer and had considerable toxicity in some patients. A critical advantage that cystine protease inhibitors have over MMPIs is that in addition to increased expression, aberrant cathepsins also change their position from being in the lysosome to moving onto the cell surface. The tumour environment is acidic so the cathepsins can work outside the cell. This may allow differential targeting of tumour-specific cathepsins through inhibitor design towards the tumour microenvironment. For example, inhibitors which are poorly cell permeable may prove advantageous as they would leave cathepsins that function normally untouched.[11]

Some cathepsins have been shown to have a role in acquired radiation and chemotherapy resistance and their inhibition has improved the outcome of such treatments.[9] Furthermore, whist cathepsins can exhibit tumour-promoting activity, there are also cysteine cathepsins which have shown tumour supressing activity, highlighting the need for higher selectivity.

1.4 Cysteine proteases in parasitic infections:

Cysteine proteases are fundamental to the metabolism of many tropical parasites and cysteine protease inhibitors have been shown to stop parasitic infections both in cell cultures and animal models.[12]

Chagas disease is the leading cause of heart disease in South America, causing over 15.000 deaths each year and it is caused by the protozoan parasite *Trypanosoma cruzi*.[13]
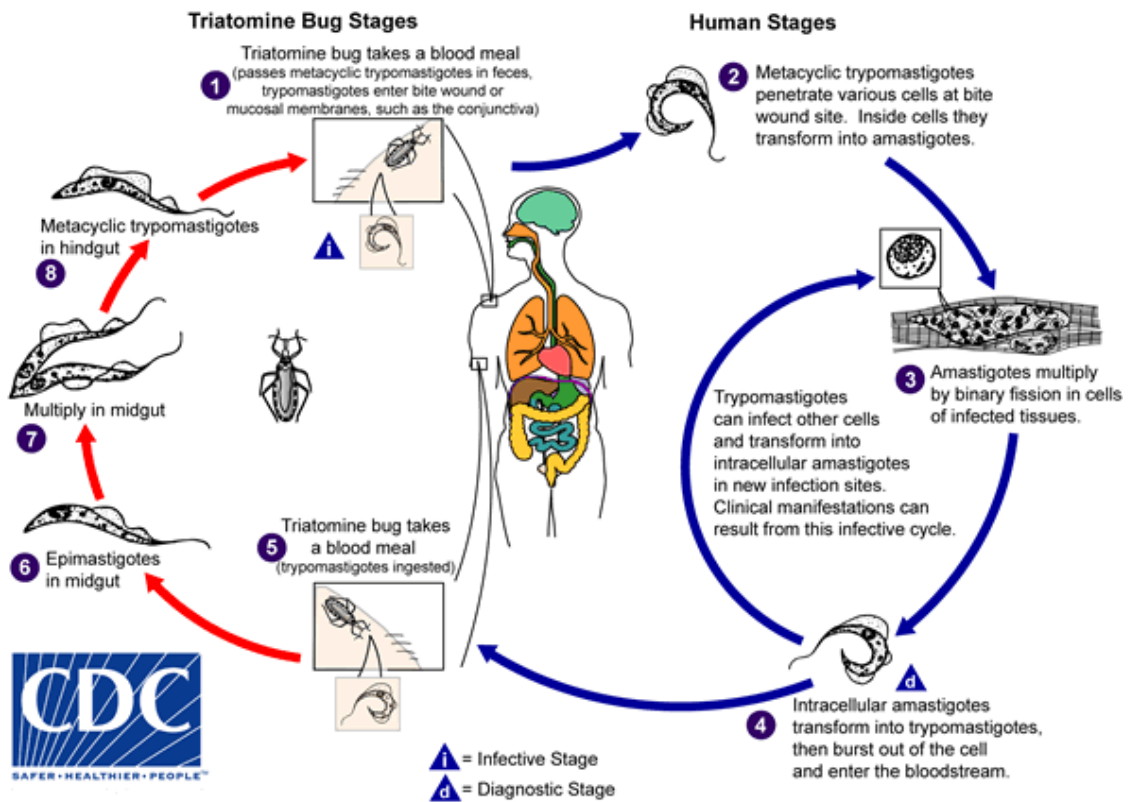
Figure 3: Life cycle of Chagas disease (https://www.cdc.gov/parasites/chagas/biology.html).

The cysteine protease Cruzain is essential for *T. cruzi* as it is involved in all stages of the parasite's life cycle (Figure 3) – infection, growth, nutrition and immune system evasion.[14] An advantage of cysteine protease inhibitors is that by selectively targeting Cruzain, the infection can be stopped at any stage during its life cycle, not only when its most infective. The World Health Organisation (WHO) recommended two drugs for the treatment of the disease: nifurtimox and benznidazole (Figure 4). However, they are less effective once the infection reaches the chronic phase and display severe side effects.[15]

Figure 4: Structures of Benznidazole and Nifurtimox.

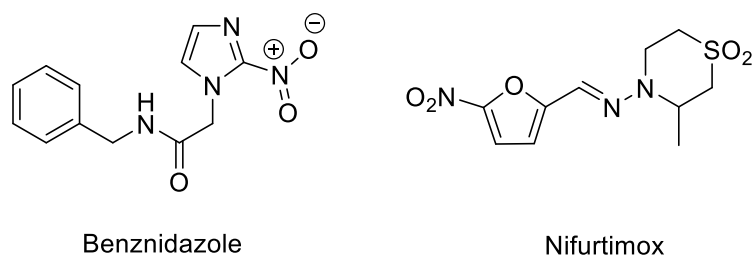K11777 (Figure 5) is a vinyl sulfone inhibitor that has shown good efficacy in mouse and dog models, low toxicity, and selectivity towards Cruzain over mammalian cysteine proteases.[16] It is also important to note that K11777 achieved the removal of both parasite adult worms and drastically reduced the quantity of eggs present in the liver and spleen, proving that a protease inhibitor can target the parasitic infection regardless of the stage in its lifecycle.[2] A factor contributing to K11777's high efficacy is that Cruzain has a strong preference for large hydrophobic residues in the P2 position, as this determines specificity by interacting with the S2 binding pocket of the cysteine protease family. Furthermore, although the P3 position is of little importance to binding, modifying it influences a number of properties including hepatotoxicity, lipophilicity and pharmacokinetics. It was determined that including the N-methylpiperazine in the P3 position would increase the bioavailability by increasing absorption in the small intestine.
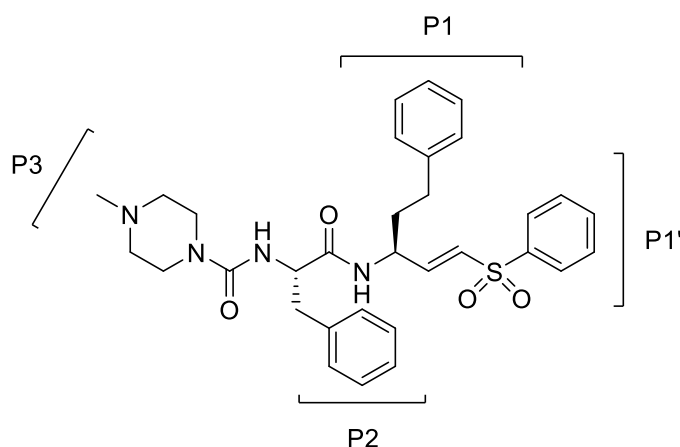

Figure 5: Structure of K11777

1.5 Current inhibitors:
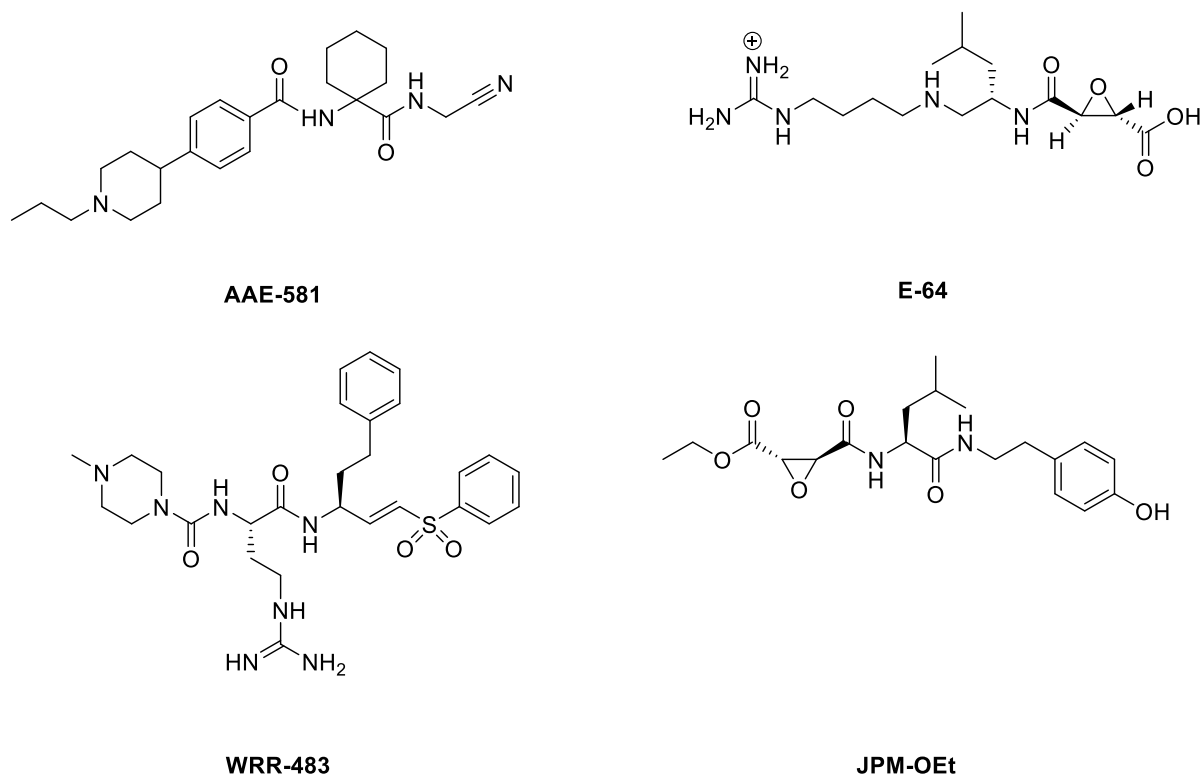
Figure 6: Structures of currently used inhibitors: nitrile (AAE-581), epoxysuccinyl (E-64, JPM-OEt), vinyl sulfones (WRR-483).

Several small molecules have been designed to selectively target and inhibit the activity of cysteine proteases. The main classes of inhibitors that have been tested on animal models and in clinical trials are nitriles, vinyl sulfones and epoxysuccinyl-derived molecules.[1] These can be either broad spectrum inhibitors or specific for particular members of the cysteine protease family. Many of these inhibitors are composed of a "backbone" that confers specificity for the required cysteine protease type and an electrophilic warhead that can react with the active site thiol. Figure 6 shows some of the inhibitors that are most widely used. Although most of these inhibitors show promising activity *in vitro*, when tested *in vivo* they were not as effective. For example, Cathepsin K inhibitors such as AAE-581 accumulate in the lysosome due to their lipophilic profile and end up inhibiting off-target enzymes such as Cathepsin S.[10]

E-64 is an epoxysuccinyl based inhibitor and it was extracted from *Aspergillus japonicus*.[10] E-64 is an irreversible, broad spectrum inhibitor, which was tested on Japanese adults with muscular dystrophy, but the drug was stopped at phase III due to off-target activity. The studies showed that E-64 had good efficacy but it would also covalently bind other proteases that were closely related to the cathepsin family.[9] Further modifications to the molecule have yielded more specific and less toxic inhibitors such as JPM-OEt but they are yet to be tested in clinical trials.[17] The vinyl sulfone K11777 has shown remarkable efficacy and low toxicity in animal models and is currently undergoing clinical trials. WRR-483 is a derivative of K11777 in which the P2 residue was changed from a phenylalanine to an arginine in the hope of achieving higher selectivity. Although the attempt to make the inhibitor more selective proved successful, the overall efficacy was decreased by putting an arginine in the P2 position. Considering its potential, low toxicity and high potency, we have chosen to use vinyl sulfone inhibitor K11777 as a foundation for the design of the thiosulfonate inhibitor.

1.6 Thiosulfonates:
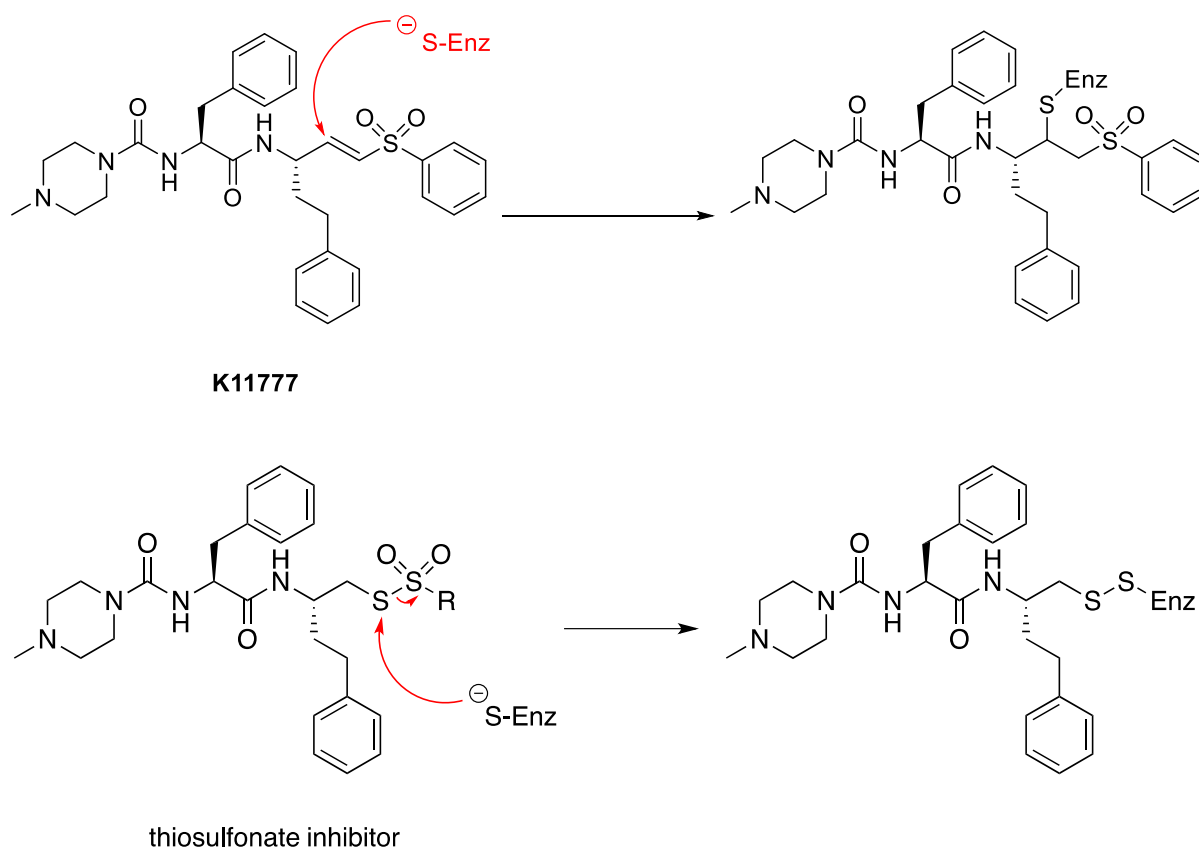
Figure 7: Mechanism of K11777 cysteine protease inhibitor compared to proposed thiosulfonate mechanism.

In this work, thiosulfonates will be explored as novel warheads for use as cysteine protease inhibitors. Methylmethanethiosulfonate (MMTS) is the simplest thiosulfonate and it is a cysteine protease inhibitor used to measure protease activity in biological assays. MMTS has also displayed anti-cancer and anti-bacterial activity.[18] A very important aspect of thiosulfonates is their selective interactions with protein thiols. This can be of great value in the synthesis of specific inhibitors. Therefore, we have chosen to include a thiosulfonate warhead in our inhibitors (Figure 7) in order to specifically target cysteine proteases over other classes of enzymes that are present in the body. Furthermore, previous work in the Liskamp group (not published) has shown that replacing the aromatic moiety in the P1' position for an aliphatic moiety in thiosulfonates enhanced the potency of the

inhibitors. This was thought to be through down-regulating the reactivity of the warhead. Taking this together with the backbone of K11777, a cysteine protease inhibitor that made it to late stage clinical trials shows potential for a successful line of inhibitors. K11777 will provide an ideal reference compound allowing conclusion to be drawn solely on the effect of the warhead and not backbone alterations.

The rationale behind the backbone design is that having N-methylpiperazine in the P3 position increases the inhibitor's assimilation in the small intestine, while the homophenylalanine side chain takes advantage of the P2 specificity of cathepsin-L like cysteine proteases, thus conferring the inhibitor specificity towards a certain member within the protease family.
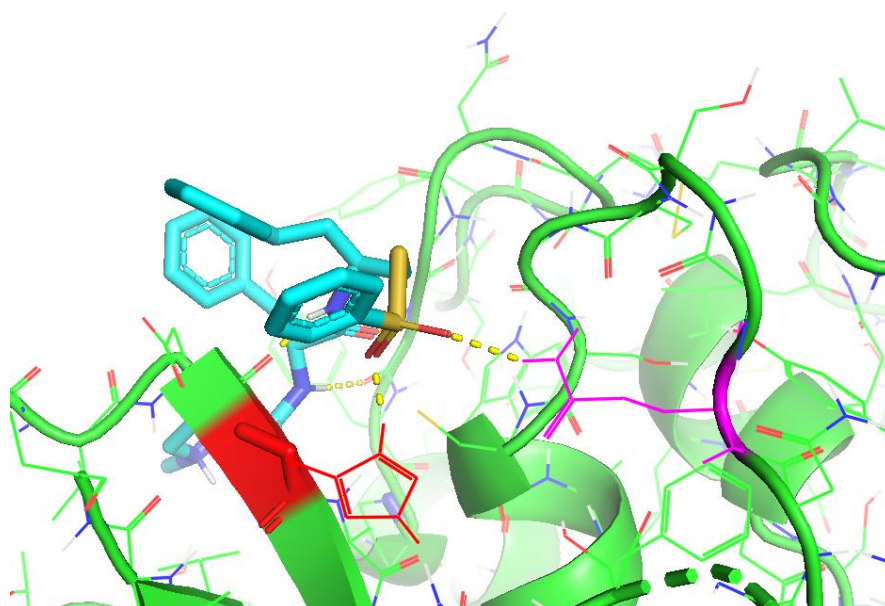
Figure 8: Thiosulfonate forming hydrogen bonds to His[159] (shown in red) of the cysteine protease active site.

The novel thiosulfonate warheads build on this specificity as other enzymes such as serine and threonine proteases have a nucleophilic oxygen in their active site. These oxygen-centred nucleophiles are hard nucleophilic centres while the active site thiol of cysteine proteases offers a soft nucleophile. Thiosulfonates aim to exploit this difference as the bivalent sulphur of the thiosulfonate moiety offers a soft electrophile, thus increasing the selectivity towards the soft sulphur-centred nucleophile of cysteine proteases. Furthermore, modelling studies have shown that the hexavalent sulphur forms favourable interactions (hydrogen bonds) with His[159] of the cysteine protease active site (Figure 8).

Previous work within the Liskamp group (unpublished) has shown that improving the stability of the thiosulfonates by down-regulating their reactivity has previously been shown to increase the potency. Other methods to expand on this observation will also be explored such as further substitution of the thiosulfonate warhead on the carbon adjacent to the bivalent sulphur. The strategy is expected to decrease the rate of a nucleophilic attack on the bivalent sulphur, thus improving stability, which is expected to translate into improved potency as previous inhibitors could be degraded before reaching the target enzyme.

2 Results:

## 2.1 Exploring efficient thiosulfonate synthesis methods:

The main aim of the project was to deliver an efficient synthesis towards the warhead component which would be coupled to the inhibitor backbone later. The synthesis for this component can be seen in Scheme 1.
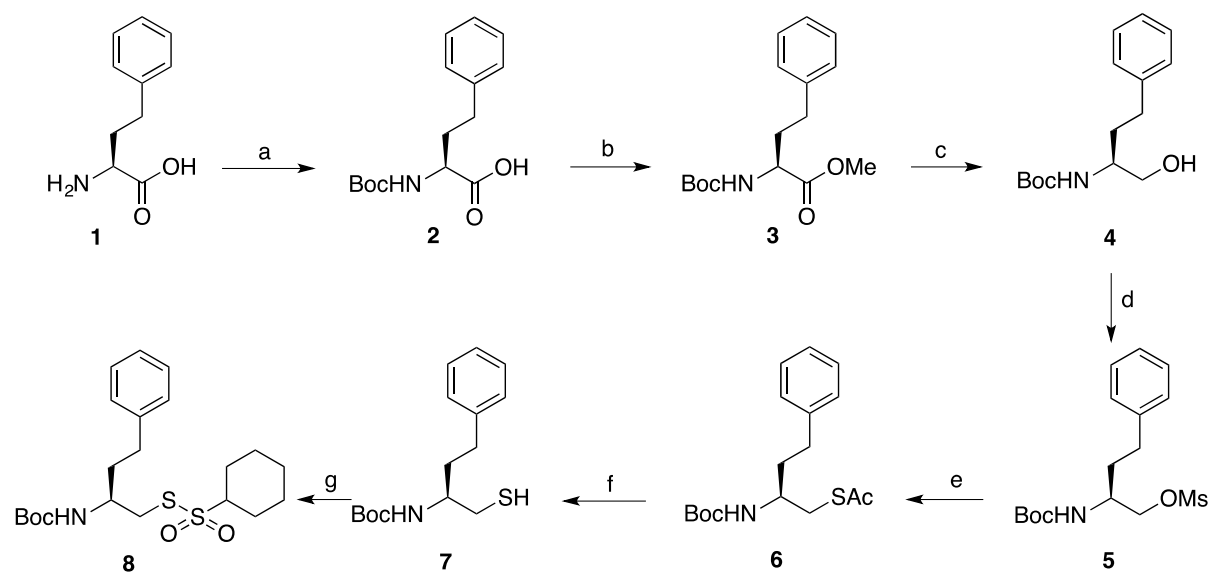
Scheme 1: Warhead synthesis: a) Boc_2O, NaOH, THF, 97%; b) MeI, K_2CO_3, DMF, 95%; c) $NaBH_4$, LiCl, EtOH, THF, 70%; d) MsCl, NEt_3, DCM, 75%; e) Cs_2CO_3, AcSH, DMF, 38%; f) $LiAlH_4$, THF, -78ºC, 94%; g) $C_{16}H_{11}BrSO_2$, DCM, 0ºC, 20%.

This method offers a quick and efficient route to the synthesis of thiosulfonate warheads that can then be incorporated in the main inhibitor via peptide coupling. By analogy to K11777, it was decided that the synthesis would be started from homophenylalanine which could be derivatised to obtain the thiosulfonate warhead along with the P1 residue. Synthesis was started from commercially available homophenylalanine **1** which was Boc protected to obtain compound **2**. The carboxylic acid was then converted to a methyl ester by alkylation under basic conditions to avoid Boc deprotection. Methyl ester **3** was then reduced to an alcohol. Following this, a functional group transformation converting alcohol **4** to a good leaving group was required, hence mesylation to **5** was chosen. The mesylate was required for a subsequent conversion to thioacetate **6** via an S_N2 reaction that would

introduce the sulphur functionality. At this stage, the thioacetate needed to be converted to a thiol. Initially, hydrolysis using EtOH, KOH and 2% water was attempted. This method yielded disulphide **9** as the major by-product (scheme 2) due to oxidation of the free thiol by atmospheric oxygen. Although all efforts were made to exclude oxygen from the reaction, it was determined that the basic conditions were accelerating this unwanted side reaction. Thus, as avoiding these conditions may improve the yield, reduction utilising $LiAlH_4$ was used.
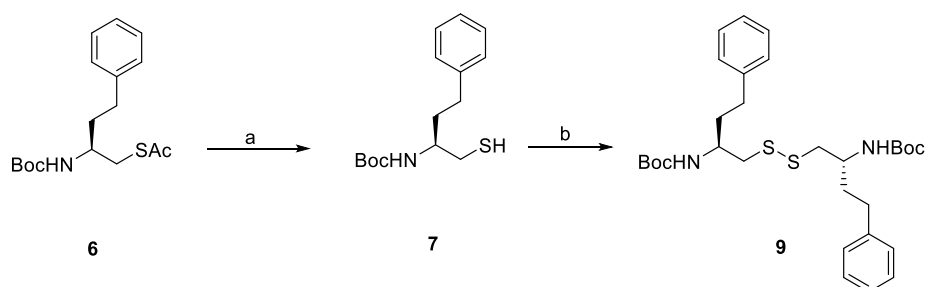
Scheme 2: Optimising thioacetate to thiol conversion to avoid undesired disulphide formation: a) EtOH, KOH, 2% water, 20% **7** and 80% **9**. b) unwanted disulphide bond formation.

The reduction using $LiAlH_4$ was successful with a 94% yield and was kept in the final synthetic route. The final step (scheme 1, g) is crucial to the synthesis as it forms the aliphatic thiosulfonate. Previously, sulfonyl chlorides were explored within the Liskamp group for this reaction, but it was found that this formed the symmetrical disulphide **12** as the major product, as shown in Scheme 3.
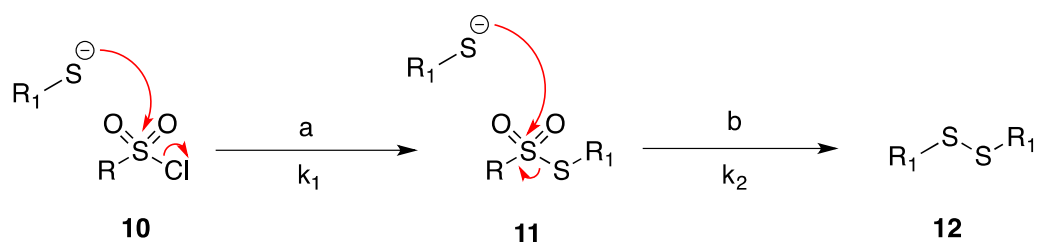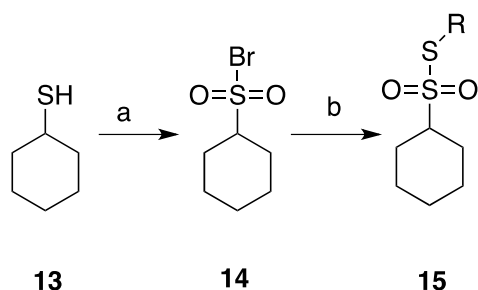

Scheme 3: Thiosulfonate formation using sulfonyl chlorides; a) DCM, DiPEA, 0°C, b) unwanted side reaction with second equivalent of thiol.

It was hypothesised that this unwanted side-reaction is happening because the rate of formation of disulphide (step b, k_2) is faster than the rate of thiosulfonate formation

(step a, k_1). Thus, sulfonyl bromides were introduced to try and increase the rate of k_1 relative to k_2, and favouring formation of thiosulfonate over disulphide. The use of sulfonyl bromides yielded a higher conversion to thiosulfonate with trace amount of disulphide by-product. With a successful, high yielding synthesis towards aliphatic thiosulfonates, we envisioned the final step (scheme 1, g) could be optimised to a one pot reaction allowing rapid expansion of the substrate scope.

Initially, it was hypothesised that the conditions in scheme 4 would be possible for sulfonyl bromide formation *in situ* and the introduction of the thiol in a one pot manner. If this proved to be successful, then substrate scope could be rapidly expanded in a one pot manner by varying the thiol starting material to generate a range of sulfonyl bromides *in situ*.

Scheme 4: One pot cyclohexane thiosulfonate formation; a) NBS, 2M-HBr, MeCN; b) addition of RSH.

The one-pot method was attempted with the conditions shown in scheme 4. However, this yielded only trace amount of thiosulfonate and symmetrical disulphide as the major product. It was thought that this was due to the sulfonyl bromide being formed too slowly or not at all and so reaction conditions were screened as shown in table 1. Using conditions presented in entry 1, symmetrical disulphide of the starting thiol was observed as the major product. At first, this was thought to happen due to the fact that the sulfonyl bromide is not being formed prior to the addition of thiol.
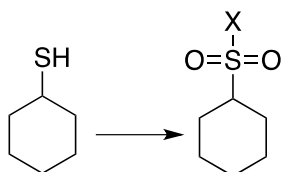
Entry	Reaction conditions	Sulfonyl halide Yield (%)
1	NBS (3 eq.), 2M-HBr (2% vol.), MeCN	25 - 30
2	NBS (4 eq.), 2M-HBr (2% vol.), MeCN	15 - 20
3	NBS (4 eq.), MeCN: H_2O (50:50)	-
4	Oxone (2.5 eq.), KBr (1 eq.), MeCN	trace
5	Oxone (3.5 eq.), KBr (1 eq.), MeCN	15 - 20
6	Oxone (1.5 eq.), KBr (0.5 eq.), MeCN	trace
7	Oxone (2.5 eq.), KBr (1 eq.), MeCN, DiPEA	-
8	Oxone (2.5 eq.), KI (1 eq.), MeCN	-

Table 1: Scanning conditions for sulfonyl halide.

The number of equivalents of NBS was increased in order to ensure that the sulfonyl bromide was properly formed before the addition of the thiol (table 1, entry 2). As this was met with limited success, it was thought that the thiol was being oxidised by the extra equivalents of oxidant added. Hence, as presented in entry 3, we eliminated the acid. This was done in consideration to the fact that the NBS supplies oxidant/bromide and H_2O is the oxygen source. Hence, it was assumed there is no need for acid in the mechanism. However, this caused the sulfonyl halide to not be formed at all, implying that the acid was required for successful bromination and sulfonyl bromide formation.

As multiple mechanisms can be drawn to produce the sulfonyl bromide under the previously mentioned conditions, reaction control through regulation of number of

equivalents was difficult to achieve. As excess oxidant could instantly oxidise the second thiol upon addition, other oxidants with a more specific mechanism were considered.

A literature review found Oxone[20] (KHSO$_5$) as an oxidant which may be suitable for the transformation of thiols to sulfonyl bromides. Upon examination of the mechanism presented in scheme 4, it can be seen that the advantage of this method is that the outcome could be, in theory, easily controlled by varying the amount of oxidant/reagents. Furthermore, the desired sulfonyl halide is produced while the symmetrical disulphide **18** is being consumed as part of this cycle. Thus, even if the unwanted side-reaction produces symmetrical disulphide (as in Scheme 3, b), this will be consumed with the addition of Oxone and KX. So, by carefully controlling the equivalents of oxidant and acid added, we can eliminate undesired disulphide by-products formed through oxidation of the second thiol by excess oxidant. Oxone reacts with the KX to produce hypohalous acid (HOX). Next, the hypohalous acid reacts with the unreacted thiol to produce a sulfinyl halide **17** which then reacts with another equivalent of thiol and is converted to disulphide **18**. The disulphide reacts with one equivalent of hypohalous acid to give compound **19** which reacts with another equivalent of HOX to form **20.** Compound **20** then rearranges to the symmetrical thiosulfonate **21**. This can then react with a second equivalent of KX and form the sulfonyl halide **22** which we need for our one pot procedure. As can be seen from the mechanism, for every two equivalents of Oxone and one equivalent of potassium halide added to the reaction, we get one equivalent of HOX. Tuning the number of equivalents of oxidant added, we can ensure that upon addition, the second equivalent of thiol will not be instantly oxidised to the symmetrical disulphide upon addition. Work started with addition of the equivalents used cited by Madabhushi et al (entry 4, table 1) but this only yielded trace sulfonyl halide. The next logical step was to add more equivalents of Oxone (entry 5) and acid so that the reaction goes all the way to compound **22**. This gave a 15-20% yield for sulfonyl halide formation in separate steps but only trace amount of product when attempted in a one pot reaction.

Considering that the quantity of KX determine the amount of HOX going into the reaction, the amount of potassium halide used to test how this would influence the outcome (entry 6). Only trace amounts of sulfonyl halide were observed meaning, in this case, at least one equivalent of KX is required to form the sulfonyl halide.

Next, DiPEA was added in an attempt to increase the nucleophilicity of the second thiol, and thus increase the reaction rate of thiosulfonate formation and avoid thiol oxidation due to excess oxidant. This reaction only yielded trace amounts of sulfonyl bromide. Next, the use of iodide for the formation of the thiosulfonate was attempted in order to increase the leaving group ability hence reaction rate in an effort to increase the formation of thiosulfonate with respect to competing side reactions. As presented in entry 8, when Oxone and potassium iodide were used, neither sulfonyl iodide or starting material were observed. Finally, since most of the changes proved to be unsuccessful or hard to trace/follow, the initial conditions were kept, and the reaction was done in separate steps.

$$2KHSO_5 + KX \longrightarrow KOH + HOX + K_2S_2O_8$$
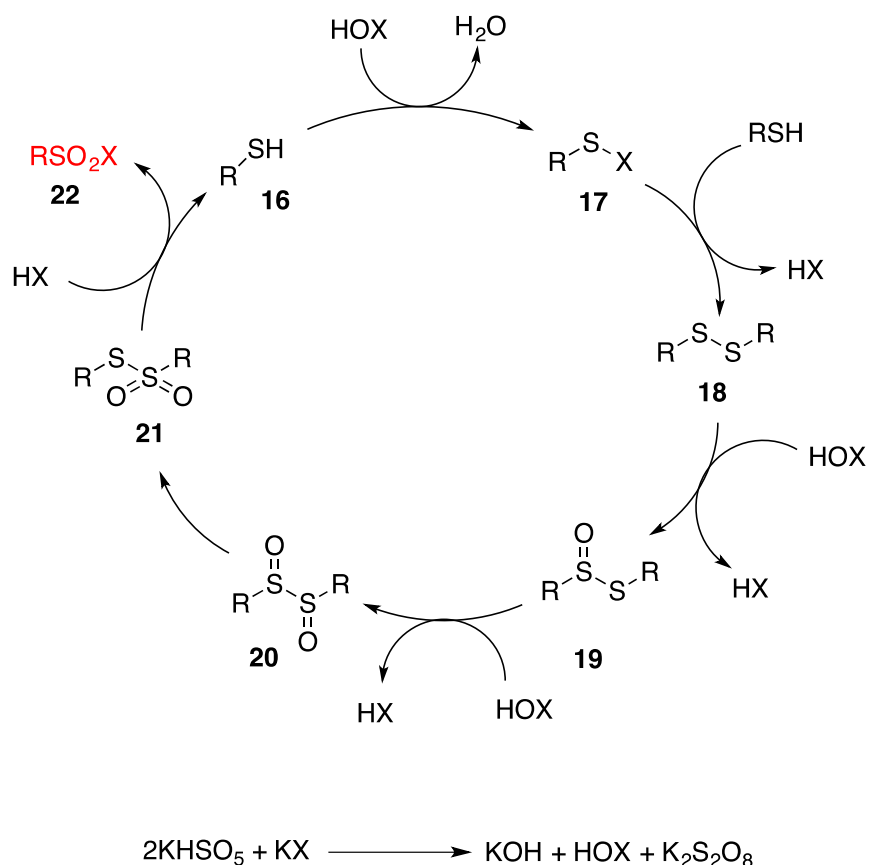
Scheme 5: Mechanism of sulfone formation upon oxidation with Oxone.

Although the route provided in scheme 1 was successful for cyclohexane thiol warhead, when it was used to prepare the cyclopentane thiol, symmetrical disulphide was observed as a main product and only trace amounts of the desired warhead was

obtained. The reasons for this observation are not yet clear as the chemistry of the cyclopentane and cyclohexane systems was not thought to differ drastically.

Cuevas et al[21] describe a method of making sulfonyl halides by using iPrOH as a source of oxygen. However, the use of iPrOH makes filtering of the product inefficient and other methods of purification proved unsuccessful and no clear product could be identified.

Moving forward, it was decided to try and obtain the thiosulfonate by using a sulfinate salt with the aim of applying this to a wider substrate scope, as the sulfonyl bromides were only efficient when generating the cyclohexane derivative. The advantage of this method is the increased stability of the sulfinate salt over the sulfonyl bromide, making it potentially easier to work it. Furthermore, the starting material is now the symmetrical disulphide rather than the thiol, meaning the strict anaerobic conditions are not required to ensure the thiol is not oxidised to an unwanted disulphide. The reduction of sulfonyl chloride with Na_2CO_3 and $NaHCO_3$ was carried out at 50ºC and the mixture was allowed to stir for 30 mins. Next, sulfonyl chloride was added followed by the disulphide. The reaction was allowed to stir overnight, and an ^1H NMR spectrum of the product was obtained but no thiosulfonate was observed.
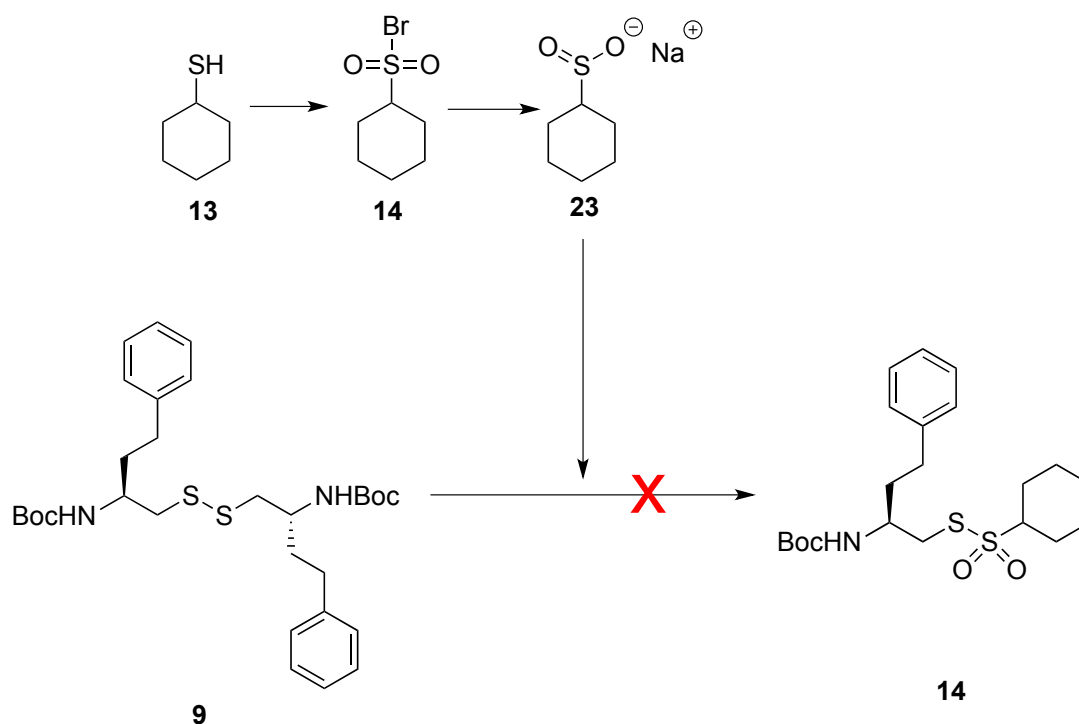
Scheme 6: Sulfinate salt method: a) NCS, 2M-HCl, MeCN; b) Na_2SO_3, $NaHCO_3$, 50ºC

2.2 Methyl warhead design:

Based on the arguments above, alternative methods to modify the thiosulfonate warhead were pursued. Rather than expanding the substrate scope at the primed side, focus now turned towards controlling reactivity by steric control. Previous work within the Liskamp group (not published) found that the thiosulfonate warhead is highly tuneable and aliphatic analogues are the most promising due to their decreased reactivity profiles. To push this concept further it was suggested that introduction of a methyl substituted in the position adjacent to the bivalent sulphur might decrease the rate of nucleophilic attack, and thus increasing the stability of the inhibitor. The increase in stability is anticipated to be met with an increased in potency as this trend has been observed in previous work done within the Liskamp group (not published).

The synthesis used D-threonine as a starting point. This amino acid is commercially available, cheap and the easy functionalisation of the carboxylic acid opens up a wide range of possibilities in terms of non-natural amino acids for future warhead design. In this instance, the final compound was desired to have a homophenylalanine side chain. To achieve this, the carboxylic acid was converted into a methyl ester (step **a**, scheme 7). Next, the amine and alcohol functionalities were protected using Boc and TBDMS respectively, yielding compound **27**. Reduction of the methyl ester directly to an aldehyde using DIBAL-H in a controlled manner was attempted. This reagent had no effect and only starting material could be observed even with extra equivalents of DIBAL-H. Consequently, it was decided to reduce the methyl ester to a primary alcohol **28** using LiAlH$_4$ and then oxidise to aldehyde **29** using Swern conditions.

The resulting aldehyde was checked by use of LCMS and TLC and the purity was sufficient for addition in the subsequent Wittig reaction. Due to time constraints, the synthesis will be carried further by a MSci student, but the subsequent steps will be briefly discussed.

With compound **30** in hand, the next step will be the hydrogenation of the alkene to an alkane, providing the key building block of homophenylalanine with a single methyl substituent next to the alcohol functionality. This will be followed by TBAF removal of the TBDMS protecting group to yield the secondary alcohol **31**. Next, the

mesylate functionality will be installed to provide a good leaving group for the next step of the synthesis. Following this, the thioacetate moiety will be introduced and reduced to give the corresponding thiol **34**, which can be coupled to a sulfonyl halide to form the thiosulfonate warhead **35**.
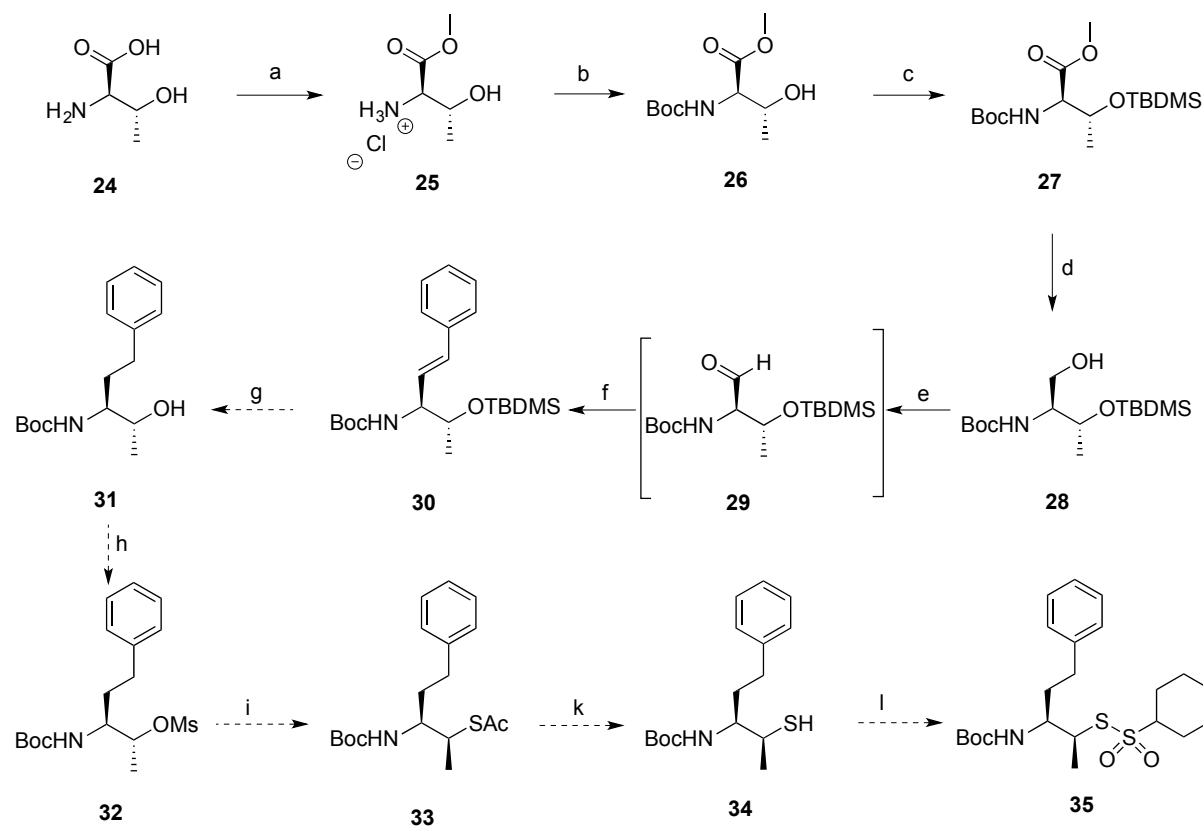

Scheme 7: Synthesis route for methylated warhead: a) Thionyl chloride, MeOH, 70°C, 2h, 95%; b) Boc$_2$O, DiPEA, DMF, 95%; c) TBDMS-Cl, Imidazole, DMF, 3h, 25%; d) LiAlH4, dry THF, -78°C, 95%; e) Oxalyl chloride, DMSO, Triethylamine, -78°C, dry THF; f) Triphenyl phosphine ylide, dry DCM, product formation observed by LCMS; g) H$_2$, Pd/C; h)MsCl, NEt$_3$, DCM; i) Cs$_2$CO$_3$, AcSH, DMF; k) LiAlH$_4$, THF l) Sulfonyl bromide, DCM.

2.3 Backbone synthesis:

Finally, the backbone was synthesised alongside the warhead fragment in anticipation of the final compound coupling. The backbone component was kept identical to K11777 in order to be able to draw direct comparisons between the newly synthesised inhibitors and the reference vinyl sulfone inhibitor, observing only the effect of the warhead on the overall stability and potency of the molecule. The backbone was synthesised using the route presented in scheme 8. The synthesis was started from commercially available Boc-Phenylalanine and the carboxylic acid

was converted into benzyl ester **37**. Next, the Boc protecting group was removed so that the *N*-methylpiperazine group could be installed. This was done in two subsequent steps, first using Triphosgene and NaHCO$_3$ to generate isocyanate, followed by addition of *N*-methylpiperazine. Finally, the benzyl ester was removed using hydrogen with a palladium/carbon catalyst and compound **40** was obtained.
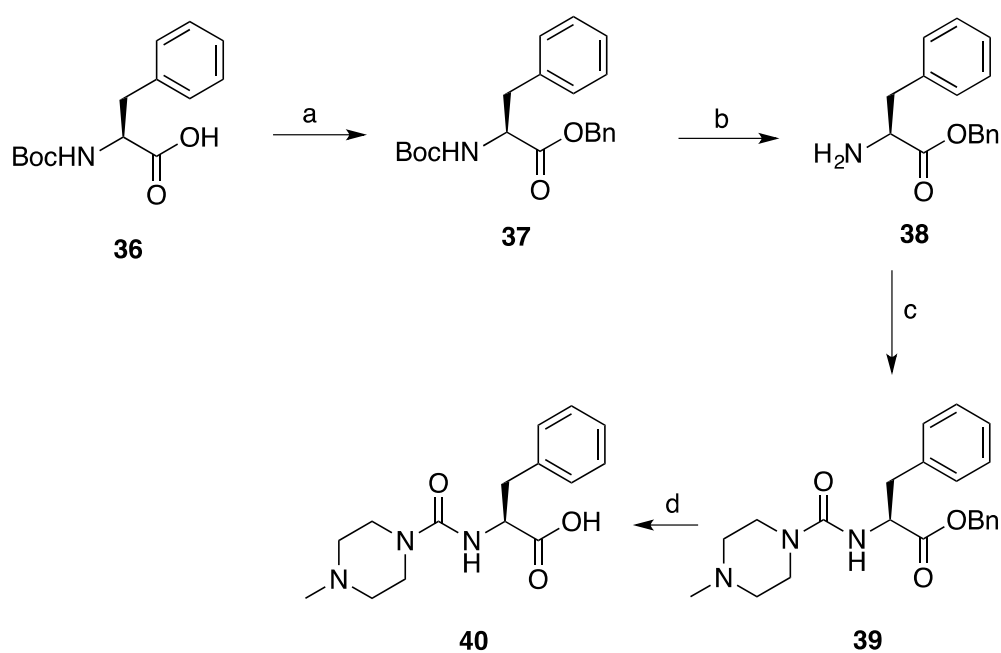
Scheme 8: Backbone synthesis: a) Benzyl bromide, K$_2$CO$_3$, DMF, 83%; b) 50% TFA, DCM, 0°C, 100%; c) Triphosgene, NaHCO$_3$, N-methylpiperazine, DCM, 0°C 70%; d) H$_2$, Pd/C, DCM, 100%.

3 Conclusions and future work:

To conclude, an efficient and reproducible synthesis towards thiosulfonates for incorporating into cysteine protease inhibitors. In an attempt to improve upon this, work was undertaken to develop a one pot aliphatic thiosulfonate synthesis method which proved unsuccessful. Thus, future work to expand the substrate scope of the aliphatic thiosulfonates will focus on the previously validated step-wise approach.

A new synthesis towards further substituted thiosulfonates, expected to enhance stability and potency of the novel warhead, has been initiated. The key methyl non-natural amino acid derived building block was isolated. This synthesis will also be applied starting from D-allo-threonine which will reverse the stereochemistry of the key methyl substituent in order to determine if this has any effect on final inhibitors.

Future work will introduce the thiosulfonate moiety into this new building block leading towards a new generation of thiosulfonate cysteine protease inhibitors.

The backbone of these inhibitor constructs has been successfully synthesised and future work will couple this with the new warhead moieties for further testing. This testing will include stability tests to determine the effect of both aliphatic substituents and further substituted methyl warhead on stability. Enzymatic testing will be carried out to correlate these results with the observed potency of the compounds and finally application to parasitic infected models will be performed.

4 Experimental:

Materials:

All reagents and starting materials were obtained from either Sigma-Aldrich® or Fluorochem Ltd. and of the highest available quality, utilized without further purification, unless specified otherwise.

All solvents were obtained from Fisher Scientific. Where necessary (under strict anhydrous conditions) solvents were obtained from a dry, distilled source. All deuterated solvents were obtained from Cambridge Isotope Laboratories, Inc. Solvents were evaporated under reduced pressure at 40°C. Reactions in solution were monitored by LCMS. Liquid chromatography mass spectrometry (LCMS) was carried out on a Thermo Scientific LCQ Fleet quadrupole mass spectrometer with a Dionex Ultimate 3000 LC using a Dr. Maisch Reprosil Gold 120 C18 column (110 Å, 3 μm, 150×4.0 mm). ^{1}H NMR data was acquired on a Bruker 400 MHz spectrometer in MeOD/CDCl$_3$ as solvent. Chemical shifts (δ) are reported in parts per million (ppm) relative to the solvent residual signal, MeOD (4.87 ppm)/CDCl$_3$(7.26 ppm). ^{13}C NMR data was acquired on a Bruker 400 MHz spectrometer at 101 MHz in CDCl$_3$/MeOD as solvent. Chemical shifts (δ) are reported in ppm relative to the solvent residual signal, MeOD (49.00 ppm). All automated column chromatography purifications were conducted with the Biotage® Isolera One® automated chromatograph. Products were purified on Biotage® SNAP Ultra cartridges pre-packed with Biotage® HP-sphereTMSpherical silica and the gradient determined by TLC plate Rf value measurement input. UV absorption was detected with Biotage® IsoleraTMSpektra UV detector at both UV1 (254 nm) and UV2 (280 nm) to identify fractions for collection.
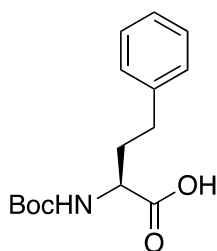
Boc-homophenylalanine (2): Homophenylalanine (25 mmol, 4.48 g, 1 eq) was dissolved in 250 mL THF and Boc_2O (30 mmol, 6.54 g, 1.2 eq) was added followed by NaOH (25 mmol, 0.99 g, 1 eq). H_2O was added to the mixture to aid the solvation of NaOH. The reaction was allowed to stir overnight, and completion was confirmed by TLC (10% EtOAc/ Pet Et). Solution was concentrated in vacuo, taken up in EtOAc, the aqueous layer was acidified to pH 4 using citric acid and washed with EtOAc (3x), Brine (1x) and dried over $MgSO_4$. The product was obtained as a colourless oil in a 97% yield. Characterization is in accordance with literature. [22]

^{1}H NMR (400 MHz, Chloroform-*d*) δ 7.47 – 7.04 (m, 5H), 5.15 (d, *J* = 8.4 Hz, 1H), 4.38 (m, 1H), 2.72 (m, 2H), 2.20 (m, 1H), 2.03 – 1.87 (m, 1H), 1.44 (s, 9H).

^{13}C NMR (101 MHz, $CDCl_3$) δ 128.48, 128.43, 126.15, 125.81, 60.53, 53.21, 34.13, 31.64, 28.32, 28.23, 27.42.
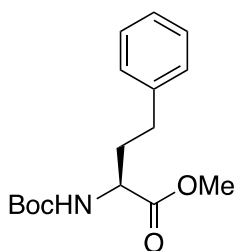

Methyl ester (3) : Compound **2** was dissolved in 250 mL DMF and MeI was added (67 mmol, 4.17 mL, 3 eq) followed by K_2CO_3 (67 mmol, 9.25 g, 3 eq). The reaction was allowed to stir for 5 hours. The solution was then concentrated in vacuo, taken up in EtOAc, the aqueous layer back extracted with EtOAc and the combined organics were washed with $KHSO_4$ (3x), water (1x), brine (1x) and dried over $MgSO_4$. The product was obtained as a colourless oil in a 95% yield. Characterization is in accordance with literature. [23]

^{1}H NMR (400 MHz, Chloroform-d) δ 7.38 – 7.01 (m, 5H), 5.08 (d, J = 8.5 Hz, 1H), 4.36 (d, J = 7.6 Hz, 1H), 3.71 (s, 3H), 2.67 (t, J = 9.4 Hz, 2H), 2.24 – 1.81 (m, 2H), 1.45 (s, 9H).

^{13}C NMR (101 MHz, CDCl$_3$) δ 129.14, 128.68, 128.47, 128.39, 126.14, 53.25, 52.25, 34.37, 31.64, 28.33, 28.24, 28.04.

LC-MS: RT (min): 6.93 (ESI-MS (m/z): 293.50 [M+H]$^+$.
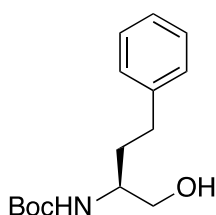
Alcohol (4): Compound **3** was dissolved in 105 mL EtOH and LiCl (65 mmol, 2.80 g, 2.5 eq) was added followed by 75 mL of THF (3 mL/mmol). Finally, NaBH$_4$ (65 mmol, 2.48 g, 2.5 eq) was added and the reaction was allowed to stir overnight and followed by TLC. The solution was then quenched with NH$_4$Cl and diluted with EtOAc. The aqueous was back extracted with EtOAc (3x), washed with brine (1x) and dried over MgSO$_4$. Product was obtained as a yellow oil in a 70% yield. Characterization is in accordance with literature. [24]

^{1}H NMR (400 MHz, Chloroform-d) δ 7.18–7.30 (5H, m), 4.64 (1H, s), 3.56–3.71 (2H, m), 2.65–2.73 (2H, m), 2.22 (1H, s), 1.74–1.86 (2H, m),1.82 (1H, m), 1.45 (9H, s).

^{13}C NMR (101 MHz, CDCl$_3$) δ 128.51, 128.48, 128.33, 126.02, 125.91, 66.02, 52.60, 33.28, 32.40, 28.82, 28.39, 28.24.

LC-MS: RT (min): 6.31 (ESI-MS (m/z): 265.67 [M+H]$^+$.
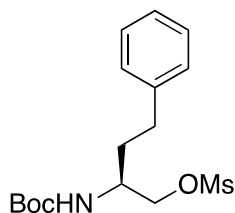
Mesylate (5): Alcohol **4** was dissolved in 150 mL DCM and Triethylamine (20 mmol, 2.83 mL, 5 eq) was added dropwise and the reaction was allowed to stir for 15 mins. Methylsulfonate chloride (15 mmol, 0.93 g, 3 eq) was added and the reaction was stirred for 1 hour and followed by TLC (50% EtOAc/Pet Et). Upon completion, the solution was concentrated in vacuo, taken up in EtOAc, washed with $KHSO_4$ (3x), the aqueous was back extracted with DCM (3x), combined organics were washed with brine (1x) and dried over $MgSO_4$. The product was obtained as a colorless oil in a 75% yield.

^{1}H NMR (400 MHz, Chloroform-*d*) δ 7.45 – 6.99 (m, 5H), 4.81 – 4.50 (m, 1H), 4.21 (d, 7.5 Hz, 2H), 3.87 (s, 1H), 3.00 (s, 3H), 2.86 – 2.58 (m, 2H), 1.87 (m, 2H), 1.46 (s, 9H).

^{13}C NMR (101 MHz, CDCl$_3$) δ 128.57, 128.43, 128.37, 126.22, 126.18, 71.13, 37.34, 33.00, 32.09, 28.48, 28.35, 28.14.
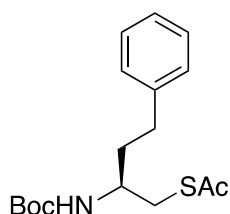
Thioacetate (6): Cs_2CO_3 (10 mmol, 3 g, 1eq) was dissolved in 100 mL DMF and Thioacetic acid (20 mmol, 1.32 mL, 2eq) was added under N_2 atmosphere and allowed to stir for 10 minutes. Mesylate **5** was dissolved in minimal amount of DMF and added to the mixture. The flask was covered in aluminum foil and the reaction was stirred for 3 hours. Upon completion, the solution was concentrated in vacuo, taken in up EtOAc, washed with water (3x), brine (1x) and dried over $MgSO_4$. Purification by column chromatography (0 -> 10% EtOAc/Pet Et) yielded the desired

product as a dark red oil in a 38% yield. Characterization is in accordance with literature. [25]

^{1}H NMR (400 MHz, Chloroform-d) δ 7.40 – 7.01 (m, 5H), 4.53 (d, 1H), 3.80 (br s, 1H), 3.21–3.01 (m, 2H), 2.75–2.60 (m, 2H), 2.35 (s, 3H), 1.87–1.74 (m, 2H), 1.45 (s, 9H);

^{13}C NMR (101 MHz, CDCl$_3$) δ 128.44, 128.36, 128.25, 125.98, 125.70, 36.45, 36.19, 33.94, 32.36, 30.58, 28.78, 28.38, 28.00.
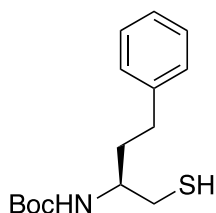

Thiol (7): Thioacetate **6** was dissolved in dry THF and the solution was cooled down to 0 C. LiAlH4 (1.2 mmol, 1.28 mL, 2 eq) was added dropwise under N2 atmosphere and the reaction was followed by TLC. Upon completion, the solution was quenched with water and the solvent was evaporated to about half the volume. The solution was then diluted in EtOAc, washed with KHSO$_4$ (3x), the aqueous was back extracted with EtOAc (2x), the combined organics were washed with brine (1x) and dried over MgSO$_4$. The product was obtained as a brown oil in a 92% yield.

^{1}H NMR (400 MHz, Chloroform-d) δ 7.23 (d, J = 26.1 Hz, 0H), 4.67 (d, J = 8.6 Hz, 1H), 3.83 (dt, J = 32.3 Hz, 1H), 2.71 – 2.54 (m, 2H), 2.89 – 2.67 (m, 2H), 2.09 (s, 1H), 1.96 – 1.68 (m, 2H), 1.46 (s, 9H).

^{13}C NMR (101 MHz, CDCl$_3$) δ 128.48, 128.43, 128.35, 126.04, 125.97, 51.20, 34.95, 32.39, 29.76, 28.47, 28.40, 28.35.

LC-MS: RT (min): 7.15 (ESI-MS (m/z): 243.00 [M+H]$^+$.
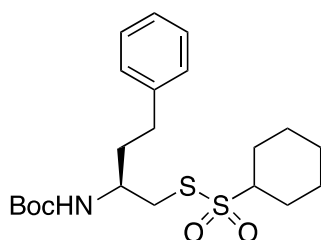
Cyclohexane warhead (8): Thiol **7** was dissolved in 15 mL DCM and the solution was cooled to 0°C. Cyclohexane sulfonyl bromide was added dropwise and the solution was removed from ice and allowed to stir at room temperature for 30 minutes. Reaction was followed via TLC (30% EtOAc/Pet Et). Upon completion, the solution was washed 3x KHSO4, the organic layers were collected, dried over MgSO4 and concentrated in vacuo. The product was obtained as a yellow oil in a 20% yield.

^{1}H NMR (400 MHz, Chloroform-*d*) δ 7.31 – 7.25 (m, 2H), 7.22 – 7.15 (m, 3H), 4.68 (d, *J* = 8.8 Hz, 1H), 3.90 – 3.82 (m, 1H), 3.39 (dd, *J* = 13.4, 4.1 Hz, 1H), 3.18 (dd, *J* = 13.8, 7.0 Hz, 1H), 3.17 – 3.11 (m, 1H), 2.68 (dtd, *J* = 16.2, 13.9, 7.4 Hz, 2H), 2.31 – 2.22 (m, 2H), 1.91 (ddt, *J* = 11.5, 4.7, 2.2 Hz, 2H), 1.87 – 1.76 (m, 2H), 1.75 – 1.67 (m, 1H), 1.63 – 1.49 (m, 2H), 1.46 (s, 9H), 1.37 – 1.26 (m, 2H), 1.26 – 1.15 (m, 1H).

^{13}C NMR (101 MHz, CDCl$_3$) δ 155.36, 140.96, 128.53, 128.38, 126.14, 79.76, 71.37, 50.06, 41.17, 35.88, 32.26, 28.38, 26.36, 26.21, 25.17, 25.11, 25.04.

LC-MS: RT (min): 5.64 (ESI-MS (m/z): 428.61 [M+H]$^+$.
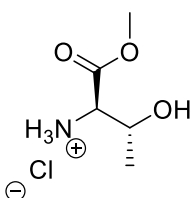
Thr-OMe (25) : D-Threonine (25 mmol, 2.97 g, 1 eq) was dissolved in 150 mL MeOH and the solution was cooled to 0 C. Thionyl Chloride (100 mmol, 7.26 mL, 4 eq) was added dropwise and the reaction was allowed to stir for 1 hour at 0 C and overnight at 70ºC under reflux. Upon completion, the solution was concentrated in vacuo and
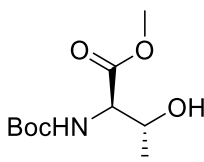
the methylated product was obtained in a 95% yield. Characterization is in accordance with literature. [26]

^{1}H NMR (400 MHz, Methanol-d_4) δ 4.30 (dd, J = 6.6, 4.2 Hz, 1H), 3.97 (d, J = 4.1 Hz, 1H), 3.87 (s, 3H), 1.35 (d, J = 6.6 Hz, 3H).

^{13}C NMR (101 MHz, MeOD) δ 64.98, 58.43, 52.33, 19.14.

[α]$_D$ = + 5.76^o

IR: 2839, 1743, 1583, 1504 cm^{-1}.

Boc-Thr-OMe (26) : Compound **25** was dissolved in 250 mL THF and Boc2O (36 mmol, 7.85 g, 1.2 eq) was added followed by the dropwise addition of DiPEA (90 mmol, 15.6 mL, 3 eq). The mixture was stirred overnight at room temperature and followed by TLC (15% EtOAc/ Pet Et). Upon completion, the solution was acidified to pH 3 using KHSO4, washed with EtOAc (3x) and dried over MgSO4. Product was obtained as a colorless oil in an 85% yield. Characterization is in accordance with literature. [27]

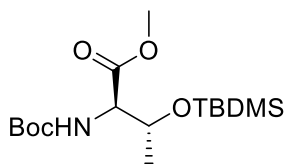^{1}H NMR (400 MHz, Chloroform-d) δ 5.47 (d, J = 9.2 Hz, 1H), 4.31 (q, J = 6.6 Hz, 2H), 3.77 (s, 3H), 2.88 (d, J = 5.4 Hz, 1H), 1.46 (s, 9H), 1.25 (d, J = 6.4 Hz, 3H).

^{13}C NMR (101 MHz, CDCl$_3$) δ 67.90, 58.80, 52.37, 28.24, 27.79, 27.34, 19.85.

LC-MS: RT (min): 5.22 (ESI-MS (m/z): 233.58 [M+H]$^+$.

[α]$_D$ = + 29.22^o

IR: 3425, 2979, 1747, 1693, 1504 cm^{-1}.

Boc-Thr-OTBDMS (27) : Compound **26** was dissolved in 150 mL of DMF and Imidazole (87.6 mmol, 6.02 g, 3 eq) was added followed by tert-Butyldimethylsilyl chloride (35 mmol, 5.27 g, 1.2 eq). The reaction was allowed to stir for 1.5 hours and was followed by TLC (10% EtOAc/Pet Et). Upon completion, the mixture was washed with diethyl ether (3x), brine (1x) and dried over MgSO4. Purification by column chromatography (0 -> 5% EtOAc/Pet Et) yielded compound **18** in a 25% yield.
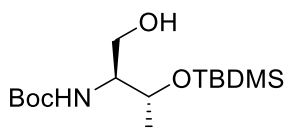
^{1}H NMR (400 MHz, Methanol-d_4) δ 4.35 (dd, *J* = 6.3, 2.5 Hz, 1H), 4.07 (d, *J* = 2.4 Hz, 1H), 3.65 (s, 3H), 1.39 (s, 9H), 1.12 (d, *J* = 6.3 Hz, 3H), 0.79 (s, 9H), 0.02 (s, 3H), -0.05 (s, 3H).

^{13}C NMR (101 MHz, MeOD) δ 68.74, 59.47, 51.35, 27.69, 27.56, 27.31, 25.25, 24.88, 24.85, 19.77, -5.54, -6.41.

LC-MS: RT (min): 8.09 (ESI-MS (m/z): 347.58 [M+H]$^+$.

[α]$_D$ = + 3.34^o

IR: 2929, 2856, 1754, 1716, 1495, 1391.

Alcohol (28) : Compound **27** was dissolved in dry tetrahydrofuran (THF) and the solution was cooled down to -78 C using dry ice/acetone. Lithium aluminium hydride (LiAlH$_4$ 1.0M in THF) was added dropwise under N$_2$ atmosphere and the solution

was allowed to stir for 1 hour and was followed by TLC (20% EtOAc/ Pet Et). Reaction completion was confirmed by LCMS and the product was obtained as a colourless oil in quantitative yield.

^{1}H NMR (400 MHz, Methanol-d_4) δ 4.11 – 3.99 (m, 1H), 3.97 – 3.85 (m, 1H), 3.53 – 3.44 (m, 2H), 1.40 (s, 9H), 1.09 (d, J = 8.3 Hz, 3H), 0.90 – 0.83 (m, 1H), 0.05 (s, 3H), 0.03 (s, 3H).

^{13}C NMR (101 MHz, MeOD) δ 65.81, 61.68, 56.92, 27.85, 27.44, 27.23, 25.13, 25.06, 24.91, 18.98, -4.86, -6.03.

LC-MS: RT (min): 7.67 (ESI-MS (m/z): 319.67 [M+H]$^+$.
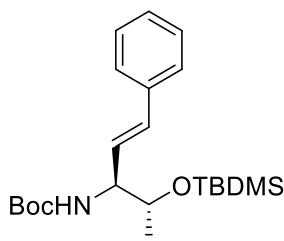
Alkene (30): Oxalyl Chloride (2.5 eq, 3.75 mmol) was dissolved in 25 mL dry DCM, cooled down to -78ºC and dry DMSO (5 eq, 7.5 mmol) was added dropwise. The solution was allowed to stir for 30 minutes, after which alcohol 19 (1 eq, 1.5 mmol) was added dropwise and allowed to stir for 45 minutes before adding NEt$_3$. The reaction was followed by TLC (20% EtOAc) and LCMS. Upon completion, the solution was diluted with DCM, washed with 1M HCl (1x), NaHCO$_3$ (1x), H$_2$O (1x) and dried over MgSO$_4$. The aldehyde was concentrated in vacuo and used directly for the Wittig reaction. The triphenylphosphine ylide was dissolved in dry THF, cooled to 0ºC, NaH (60% mineral oil, 1.2 eq, 5.1 mmol) was added and stirred for 1 hour. The freshly made aldehyde was dissolved in THF and added dropwise to the solution. Reaction was followed via TLC (20% EtOAc) and LCMS. Upon completion, the product was washed with 1M HCl (1x), Brine (1x), dried over MgSO$_4$. The product was obtained as a dark orange solid.

LC-MS: RT (min): 8.10 (ESI-MS (m/z): 392.63 [M+H]$^+$.
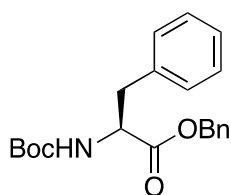
Boc-Phe-OBn (37) : Boc protected amino acid 36 was dissolved 250 mL DMF and Benzyl bromide (24 mmol, 2.85 mL, 1.5 eq) was added, followed by K_2CO_3 (64 mmol, 8.84 g, 4 eq) and allowed to stir overnight. The reaction was followed by TLC (15% EtOAc/Pet Et) and concentrated in vacuo, taken up in EtOAc, washed with water (2x), back extracted with EtOAc and dried over MgSO4. Product was obtained as colourless oil in an 83% yield. Characterization is in accordance with literature. [28]

^{1}H NMR (400 MHz, Chloroform-*d*) δ 7.42 – 7.19 (m, 10H), 5.16 – 5.07 (m, 2H), 4.98 (d, *J* = 8.5 Hz, 1H), 4.67 – 4.54 (m, 1H), 3.07 (m, 2H), 1.41 (s, 9H).

^{13}C NMR (101 MHz, CDCl$_3$) δ 129.52, 129.48, 129.41, 129.36, 128.66, 128.59, 128.27, 127.63, 126.98, 126.29, 67.11, 54.46, 38.28, 28.62, 28.31, 28.25.
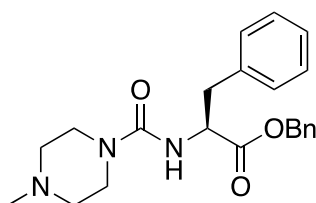
MPip-Phe-OBn (39): Compound **38** was dissolved in 100 mL DCM and 100 mL NaHCO3 were added followed by Triphosgene (6.64 mmol, 2.10 mL, 0.5 eq). The reaction was allowed to stir for 1 hour and was followed by TLC (20% EtOAc/Pet Et). 1-Methylpiperazine was added dropwise and the solution was allowed to stir overnight. Once the reaction was completed, the aqueous layer was back extracted with DCM and the combined organics were washed with Brine (1x) and dried over MgSO$_4$. Purification by column chromatography (0 -> 5% MeOH/DCM) yielded the product as a yellow oil in a 70% yield. Characterization is in accordance with literature. [29]

^{1}H NMR (400 MHz, Chloroform-*d*) δ 7.57 – 6.82 (m, 10H), 5.23 – 5.05 (m, 2H), 4.85 (s, 2H), 3.36 (d, *J* = 5.1 Hz, 4H),3.10 (m,2H) 2.38 (d, *J* = 5.2 Hz, 4H), 2.31 (s, 3H).

LC-MS: RT (min): 5.39 (ESI-MS (m/z): 381.92 [M+H]$^+$.
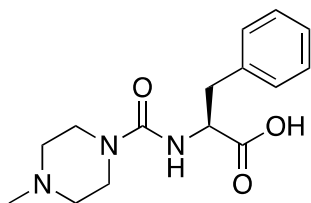
MPip-Phe-OH (40) : Compound **39** was dissolved in EtOH/AcOH (1%) and Pd/C was added under a H$_2$ atmosphere. The reaction was allowed to stir for 3 hours and the product was obtained in a quantitive yield. Characterization is in accordance with literature. [30]

^{1}H NMR (400 MHz, Chloroform-*d*) δ 7.34 – 7.11 (m, 5H), 4.56 (m, 1H), 3.74 – 3.36 (m, 4H), 3.09 (d, *J* = 7.4 Hz, 2H), 2.73 (s, 4H), 2.51 (s, 3H).

^{13}C NMR (101 MHz, CDCl$_3$) δ 129.63, 128.13, 127.11, 126.48, 126.43, 55.74, 55.23, 53.20, 44.86, 44.06, 8.59.

LC-MS: RT (min): 4.39 (ESI-MS (m/z): 291.83 [M+H]$^+$.

References:

1) Otto, H.-H.; Schirmeister, T. Cysteine Proteases and Their Inhibitors. *Chem. Rev.* **1997**, *97* (1), 133–172.

2) Abdulla, M.-H.; Lim, K.-C.; Sajid, M.; McKerrow, J. H.; Caffrey, C. R. Schistosomiasis Mansoni: Novel Chemotherapy Using a Cysteine Protease Inhibitor. *PLoS Med.* **2007**, *4* (1), e14.

3) Kerr, I. D.; Lee, J. H.; Farady, C. J.; Marion, R.; Rickert, M.; Sajid, M.; Pandey, K. C.; Caffrey, C. R.; Legac, J.; Hansell, E.; et al. Vinyl Sulfones as Antiparasitic Agents and a Structural Basis for Drug Design. *J. Biol. Chem.* **2009**, *284* (38), 25697–25703.

4) Turk, V.; Stoka, V.; Vasiljeva, O.; Renko, M.; Sun, T.; Turk, B.; Turk, D. Cysteine Cathepsins: From Structure, Function and Regulation to New Frontiers. *Biochim. Biophys. Acta - Proteins Proteomics* **2012**, *1824* (1), 68–88.

5) I. Schechter, A. Berger, On the size ofthe active site in proteases. I. Papain, Biochem. Biophys. Res. Commun. 27 (1967) 157–162.

6) Chen, Y. T.; Brinen, L. S.; Kerr, I. D.; Hansell, E.; Doyle, P. S.; McKerrow, J. H.; Roush, W. R. In Vitro and in Vivo Studies of the Trypanocidal Properties of WRR-483 against Trypanosoma Cruzi. *PLoS Negl. Trop. Dis.* **2010**, *4* (9).

7) Fabien Lecaille, †; Jadwiga Kaleta, ‡ and; Dieter Brömme*, †. Human and Parasitic Papain-Like Cysteine Proteases: Their Role in Physiology and Pathology and Recent Developments in Inhibitor Design. **2002**.

8) Kirschke, H. Cathepsin L. *Handb. Proteolytic Enzym.* **2013**, *2*, 1808–1817.

9) Olson, O. C.; Joyce, J. A. Cysteine Cathepsin Proteases: Regulators of Cancer Progression and Therapeutic Response. *Nat. Rev. Cancer* **2015**, *15* (12), 712–729.

10) Palermo, C.; Joyce, J. A. Cysteine Cathepsin Proteases as Pharmacological Targets in Cancer. *Trends Pharmacol. Sci.* **2008**, *29* (1), 22–28.

11) Joyce, J. A.; Baruch, A.; Chehade, K.; Meyer-Morse, N.; Giraudo, E.; Tsai, F. Y.; Greenbaum, D. C.; Hager, J. H.; Bogyo, M.; Hanahan, D. Cathepsin Cysteine Proteases Are Effectors of Invasive Growth and Angiogenesis during Multistage Tumorigenesis. *Cancer Cell* **2004**, *5* (5), 443–453.

12) Beaulieu, C.; Isabel, E.; Fortier, A.; Massé, F.; Mellon, C.; Méthot, N.; Ndao, M.; Nicoll-Griffith, D.; Lee, D.; Park, H.; et al. Identification of Potent and Reversible Cruzipain Inhibitors for the Treatment of Chagas Disease. *Bioorganic Med. Chem. Lett.* **2010**, *20* (24), 7444–7449.

13) Martinez-Mayorga, K.; Byler, K. G.; Ramirez-Hernandez, A. I.; Terrazas-Alvares, D. E. Cruzain Inhibitors: Efforts Made, Current Leads and a Structural Outlook of New Hits. *Drug Discov. Today* **2015**, *20* (7), 890–898.

14) Ndao, M.; Beaulieu, C.; Black, W. C.; Isabel, E.; Vasquez-Camargo, F.; Nath-Chowdhury, M.; Massé, F.; Mellon, C.; Methot, N.; Nicoll-Griffith, D. A. Reversible Cysteine Protease Inhibitors Show Promise for a Chagas Disease Cure. *Antimicrob. Agents Chemother.* **2014**, *58* (2), 1167–1178.

15) Powers, J. C.; Asgian, J. L.; Ekici, Ö. D.; James, K. E. Irreversible Inhibitors of Serine, Cysteine, and Threonine Proteases. *Chem. Rev.* **2002**, *102* (12), 4639–4750.

16) Chen, Y. T.; Lira, R.; Hansell, E.; McKerrow, J. H.; Roush, W. R. Synthesis of Macrocyclic Trypanosomal Cysteine Protease Inhibitors. *Bioorg. Med. Chem. Lett.* **2008**, *18* (22), 5860–5863.

17) Meara, J. P.; Rich, D. H. Mechanistic Studies on the Inactivation of Papain by Epoxysuccinyl Inhibitors. *J. Med. Chem.* **1996**, *39* (17), 3357–3366.

18) Reddy, B. S.; Kawamori, T.; Lubet, R.; Steele, V.; Kelloff, G.; Rao, C. V. Chemopreventive Effect of S-Methylmethane Thiosulfonate and Sulindac Administered Together during the Promotion/Progression Stages of Colon Carcinogenesis. *Carcinogenesis* **1999**, *20* (8), 1645–1648.

19) Nakamura, Y. K.; Matsuo, T.; Shimoi, K.; Nakamura, Y.; Tomita, I. *S* -Methyl Methanethiosulfonate, Bio-Antimutagen in Homogenates of *Cruciferae* and *Liliaceae* Vegetables. *Biosci. Biotechnol. Biochem.* **1996**, *60* (9), 1439–1443.

20) Madabhushi, S.; Jillella, R.; Sriramoju, V.; Singh, R. Oxyhalogenation of Thiols and Disulfides into Sulfonyl Chlorides/Bromides Using Oxone-KX (X = Cl or Br) in Water. *Green Chem.* **2014**, *16* (6), 3125–3131.

21) Silva-Cuevas, C., Perez-Arrieta, C., Polindara-García, L. A. & Lujan-Montelongo, J. A. Sulfonyl halide synthesis by thiol oxyhalogenation using NBS/NCS – iPrOH. *Tetrahedron Lett.* **58,** 2244–2247 (2017).

22) Schirmeister, T. *et al.* Quantum Chemical-Based Protocol for the Rational Design of Covalent Inhibitors. *J. Am. Chem. Soc.* **138,** 8332–8335 (2016).

23) Jackson, R. F. W., Fraser, J. L., Wishart, N., Porter, B. & Wythes, M. J. Synthesis of α-amino acids using amino acid γ-anion equivalents: Synthesis of 5-oxo α-amino acids, homophenylalanine derivatives and pentenylglycines. *J. Chem. Soc. - Perkin Trans. 1* 1903–1912 (1998).

24) Lee, K. D. *et al.* New synthesis and ring opening of cis-3-alkylaziridine-2-carboxylates. *Tetrahedron* **57,** 8267–8276 (2001).

25) Cywin, C. L. *et al.* The design of potent hydrazones and disulfides as cathepsin S inhibitors. *Bioorganic Med. Chem.* **11,** 733–740 (2003).

26) Cobb, S. L. & Vederas, J. C. A concise stereoselective synthesis of orthogonally protected lanthionine and β-methyllanthionine. *Org. Biomol. Chem.* **5,** 1031–1038 (2007).

27) Tsuji, H. & Yamamoto, H. Hydroxy-Directed Amidation of Carboxylic Acid Esters Using a Tantalum Alkoxide Catalyst. *J. Am. Chem. Soc.* **138,** 14218–14221 (2016).

28) Hatano, M. *et al.* Ligand-Assisted Rate Acceleration in Lanthanum(III) Isopropoxide Catalyzed Transesterification of Carboxylic Esters. *Org. Lett.* **13,** 426–429 (2010).

29) Rhee, S. W., Bradford, W. W., Malerich, J. P. & Tanga, M. J. Carbon-14 labeling of K777·HCl, a therapeutic agent for Chagas disease. *J. Label. Compd. Radiopharm.* **56,** 461–463 (2013).

30) Yang, P. Y., Wang, M., He, C. Y. & Yao, S. Q. Proteomic profiling and potential cellular target identification of K11777, a clinical cysteine protease inhibitor, in Trypanosoma brucei. *Chem. Commun.* **48,** 835–837 (2012).